Advances in Nano Research, *Vol. 12, No. 6 (2022) 639-652*
https://doi.org/10.12989/anr.2022.12.6.639

P3H4 promotes renal cell carcinoma progression and suppresses antitumor immunity via regulating GDF15-MMP9-PD-L1 axis

Shuo Tian[†1,2], Yan Huang[†2], Dong Lai[†1,2], Hanfeng Wang[2], Songliang Du[2], Donglai Shen[2], Weihao Chen[1,2], Yundong Xuan[1,2], Yongliang Lu[1,2], Huayi Feng[1,2], Xiangyi Zhang[2,3], Wenlei Zhao[1], Chenfeng Wang[1,2], Tao Wang[1,2], Shengpan Wu[2], Qingbo Huang[2], Shaoxi Niu[2], Baojun Wang[*2], Xin Ma[**2] and Xu Zhang[***2]

[1]*Chinese PLA Medical School, Beijing 100853, PR China*
[2]*Department of Urology, The Third Medical Centre, Chinese PLA General Hospital, Beijing 100853, PR China*
[3]*School of Medicine, Nankai University, Tianjin 300071, PR China*

(*Received January 18, 2021, Revised March 20, 2022, Accepted March 21, 2022*)

Abstract. The prolyl 3-hydroxylase family member 4 (P3H4), is associated with post-translational modification of fibrillar collagens and aberrantly activated in cancer leading to tumor progression. However, its role in clear cell renal cell carcinoma (ccRCC) is still unknown. Here we reported that P3H4 was highly expressed in renal cancer tissues and significantly positive correlated with poor prognosis. Knockdown of P3H4 inhibited the proliferation, migration and metastasis of renal cancer cells in vitro and in vivo, and also, overexpression of it enhanced the oncogenic process. Mechanistically, P3H4 depletion decreased the levels of GDF15-MMP9 axis and repressed its downstream signaling. Further functional studies revealed that inhibition of GDF15 suppressed renal cancer cell growth and GDF15 recombinant human protein (rhGDF15) supplementation effectively rescued the inhibitory effect induced by P3H4 knockdown. Moreover, decreased levels of MMP9 caused by inhibition of P3H4-GDF15 signaling constrained the expression of PD-L1 and suppression of P3H4 accordingly promoted anti-tumor immunity via stimulating the infiltration of CD4+ and CD8+ T cells in syngeneic mice model. Taken together, our findings firstly demonstrated that P3H4 promotes ccRCC progression by activating GDF15-MMP9-PD-L1 axis and targeting P3H4-GDF15-MMP9 signaling pathway can be a novel strategy of controlling ccRCC malignancy.
Keywords: ccRCC; GDF15; immunosuppression; MMP9; P3H4; PD-L1

1. Introduction

Renal cell carcinoma (RCC), one of the most common cancers of the urinary system, is insidious and difficult to diagnose and treat (Jonasch *et al*. 2021). Clear cell renal cell carcinoma (ccRCC) accounts for more than 75% of RCC, of which nearly 30% cases have local recurrence and distant metastasis after tumor resection, and the 5-year survival rate for patients with advanced ccRCC is poor (Du *et al*. 2017, Motzer *et al*. 2017, Escudier *et al*. 2019). Although targeted therapy and immunotherapy have achieved great success in clinical outcomes of patients with metastatic ccRCC, resistance to these therapeutic modalities limits the percentage of patients with long-lasting responses. Thus, elucidating the underlying mechanisms of ccRCC metastasis and finding novel clinical indicator and therapeutic target for ccRCC are urgently needed.

Growth differentiation factor 15 (GDF15), also known as macrophage inhibitory cytokine-1 (MIC-1), is a stress-responsive cytokine belonging to the TGFβ superfamily and serves an important role in regulating angiogenesis, inflammation and metabolism (Tsai *et al*. 2018, Baek and Eling 2019, Spanopoulou and Gkretsi 2020, Suriben *et al*. 2020, Lai *et al*. 2021). Growing evidences suggest that GDF15 is becoming an appealing candidate to treat many metabolic diseases such as obesity and type 1 diabetes mellitus (Day *et al*. 2019, Coll *et al*. 2020, Nakayasu *et al*. 2020). Besides, GDF15 is always upregulated in tumor cells and participates in tumorigenesis-related activities, including cell growth, migration, invasion and metastasis partly via activation of EMT pathway, Ras/PI3K pathway and so on (Lerner *et al*. 2016, Li *et al*. 2016, 2018a, 2020, Lu *et al*. 2018, Guo *et al*. 2021). Nevertheless, the role of GDF15 in renal cell cancer and the underlying molecular mechanism is largely unknown.

Matrix metalloproteinases (MMPs) are a family of zinc-dependent endopeptidases and mediate degradation of molecules for adhesion and matrix interactions (Fields 1991, 2013, Van Doren 2015). MMPs play critical role in tumorigenesis and tumor progression, invasion and metastasis (Coussens *et al*. 2002, Egeblad and Werb 2002, Roy *et al*. 2009, Kessenbrock *et al*. 2010), among them, MMP9 is a well-recognized member of MMP family (Zhou *et al*. 2014). Increased level of MMP9 has been implicated in renal tumorigenesis and malignant progression (Huang *et*

*Corresponding author, Mr.,
E-mail: baojun40009@126.com
**Co-corresponding author, Mr.,
E-mail: urologist@foxmail.com
***Co-corresponding author, Mr.,
E-mail: urology@mail.chzu.edu.cn
[†]These authors contributed equally to this work

ISSN: 2287-237X (Print), 2287-2388 (Online)

al. 2017, Yang *et al*. 2019, Yue *et al*. 2020, Dorandish *et al*. 2021). Moreover, previous studies showed that MMP2/MMP9 is involved in modulating tumor microenvironment via regulating PD-L1 levels, and MPP2/9 inhibitor treatment greatly enhances the therapeutic efficacy of PD-1 blockade (Marshall *et al*. 2015, Ye *et al*. 2020).

The prolyl 3-hydroxylase family member 4 (P3H4) (alias SC65), a kind of small molecular compounds belonging to quinone, is clarified as a protein associated with the association complex (SC) (Chen *et al*. 1992, Gruenwald *et al*. 2014, Ochs RL 2017). It's related with cerebral ischemia-reperfusion and hypertension, and gradually function of P3H4 in cancer has been elucidated (Weliky *et al*. 1975, Li *et al*. 2018b, Wan *et al*. 2018, Hao *et al*. 2020, Jin *et al*. 2021, Lee *et al*. 2021). However, the function of P3H4 in ccRCC is largely unknown. Here, we demonstrated that P3H4 was significantly upregulated in ccRCC tissues and its high expression was correlated with worse prognosis in ccRCC patients. Functional and mechanistic studies revealed that P3H4 drived ccRCC malignant behavior and mediated tumor immune-suppression via upregulating GDF15-MMP9-PD-L1 axis. Collectively, these findings indicated the clinical potential of P3H4-GDF15-MMP9 signaling axis as novel therapeutic targets for better outcomes of ccRCC patients.

2. Methods and materials

2.1 Patients and clinical samples

Human ccRCC and normal renal tissues were collected from 229 patients who were operated surgery at the Urology Department of the Chinese People's Liberation Army (PLA) General Hospital (Beijing, China) from January 2012 to December 2020. All samples of cancer tissue had been pathologically confirmed as ccRCC according to the 2011 Union for International Cancer Control TNM classification of malignant tumors. All patients were informed and signed a consent on the use of clinical specimens for scientific research. This study was approved by the ethics committee of the Chinese People's Liberation Army (PLA) General Hospital. Tissue microarray was constructed in our laboratory.

2.2 Cell lines

Human immortalized renal epithelial cell 293T and ccRCC cell lines ACHN, 786-O, Caki-1, Caki-2 and SN12 were preserved in our laboratory. Fetal bovine serum (FBS) was purchased from EVERY GREEN (Hangzhou, China). The medium of high glucose-DMEM, RPMI-1640 and McCoy's 5A were purchased from VIVICUM bioscience (Beijing, China). All the cells were cultured in medium containing 10% FBS and 1% penicillin/streptomycin at 37℃ in 5% CO2. 293TN and SN12 were cultured in DMEM. ACHN cells were cultured in MEM medium, and 786-O were cultured in RPMI-1640 medium. Caki-1 and Caki-2 cells were cultured in McCoy's 5A medium. When the cells reached 80–90% confluence, digestion and passage were performed with trypsinization.

2.3 Plasmid construction, transfection, and infection

Short hairpin RNA (shRNA) sequences targeting human P3H4, oligonucleotides were designed and synthesized by BGI (Shenzhen, China) and cloned into pLKO.1 vector. The expressions of GDF15 were silenced with siRNA oligonucleotides. Overexpression of P3H4 plasmids were designed by BGI.

Lentivirus were generated in 293T cells. Cells were transfected with 6 μg vector plasmids and 4.5 μg psPAX2 and 1.5 μg pMD2-VSVG using the standard calcium chloride transfection method. Calcium transfection kit was purchased from Macgene Biotech (Beijing, China). 48 h and 72 h after transfection, viral supernatant containing released viruses was collected and filtered through 0.45 μm filter. Target cells were infected with virus and 10 ug/ml polybrene for 24 hours. Later, infected cells were selected with 2 μg/mL puromycin (Sigma, USA) for three or four days until they were stable.

Knockdown of P3H4 plasmids were transfected into SN12 and Caki-2 cells with 72 hours. Knockdown of GDF15 plasmid was transfected into SN12 cells. Overexpression of P3H4 plasmids were transfected into Caki-1 cells.

2.4 Western blot

Cells were lysed on ice for 30 minutes supplemented with RIPA buffer plus phosphatase inhibitors and protease inhibitors. After centrifugation with 12,000 r.p.m. for 15 minutes at 4°C, the liquid supernatant was collected for protein concentration quantification (BCA methods). For western blot analysis, 20 μg of protein extracts were loaded to 10% sodium dodecyl sulfate-polyacrylamide gel electrophoresis gels and transferred to nitrocellulose membranes. To prevent non-specific binding of antigens, the membrane was incubated with 5% bovine serum albumin in TBST buffer for 1 h at room temperature. Different regions were picked with primary antibodies against P3H4 (Proteintech, #15288-1-AP), GDF15 (Proteintech, #27455-1-AP), and MMP9 (Proteintech, #10375-2-AP) overnight at 4℃. β-actin was used as a loading control. After cleaning three times with TBST buffer for 5 minutes each time, the membranes were incubated with HRP-conjugated secondary antibodies for 1 h at 37℃ temperature. The target proteins were visualized with Super ECL Detection Reagent (Thermo Fisher Scientific). The information of antibodies was listed in Supplementary Table 1.

2.5 RNA extraction and qRT-PCR

TRIzol reagent (Invitrogen) was used to extract total RNA. Complementary DNA was synthesized with ProtoScript® IIFirst-Strand cDNA Synthesis Kit (E6300S, NEB, USA) according to the manufacturer's instruction. Afterwards, the mRNA expression levels of genes were detected with NovoStart® SYBR Green SuperMix Plus (E096-01A, novoprotein, China). Relative mRNA expressions were normalized to peptidylprolyl isomerase A (PPIA) with the $2^{-\Delta\Delta CT}$ method. The primer sequences used are listed in Supplementary Table 1.

Table 1 P3H4 expression was associated with clinicopathological parameters in ccRCC

Clinicopathological parameters	n	P3H4 expression		P
		Low	High	
Gender				
Male	156	101	45	0.019
Female	70	37	33	
Age (years)				
<65	166	106	60	0.098
≥65	60	31	20	
Tumor diameter (cm)				
<4	72	33	39	0.002
≥4	154	39	115	
Fuhrman				
1-2	199	177	22	0.001
3-4	27	12	15	

2.6 RNA-sequence(seq) analysis

Total RNA was extracted from cells using TRIzol reagent and sent to BMK Corporation. The heatmap was performed by BMKCloud, and the phyper function of R software is used for enrichment analysis to calculate the P value, and then perform FDR correction on the P value. Q value < 0.05 is regarded as significant enrichment.

2.7 Primary renal cancer cell culture

Tumor specimens from two renal cell cancer patients were isolated with collagenase digestion and transported to the lab within 10 min. After removing blood clots, the samples were rinsed with sterile phosphate-buffered saline (PBS) twice and cut into small fragments in a size of about 1 mm^3. Then, the fragments were incubated with collagenase of 1% (Solarbio) in a gently shaking water bath. After incubation with collagenase, the rest of samples were collected and put into 24 well plates. Cells were isolated and divided for culture using F medium containing 25% Ham's F-12 nutrient mix (Thermo Fisher Scientific, Carlsbad, CA) supplemented with 10% FBS.

2.8 Immunohistochemical staining

For P3H4/GDF15/MMP9 staining, tissue microarrays were obtained from the tissue bank at Urology Department of the Chinese PLA General Hospital, Beijing, China. IHC was performed on the samples from the human RCC tissues and mouse xenografted tumors, as described previously. In brief, paraffin tissue sections were deparaffinized by xylene, rehydrated using graded ethanol, and blocked with 3% hydrogen peroxide for eliminating endogenous peroxidase activity, after which tissue sections were incubated with primary antibodies. Then, HRP-conjugated secondary antibody and DAB substrates were used for staining. IHC staining score analysis was used to figure the cases with high or low expression of targeted protein. The expression was assessed as follows: the percentage of positive cells was scored as 1, <25%, 2, 25–50%, 3, 50–75%, 4, >75% and the intensity of IHC staining was scored as 0, negative, 1, weak, 2, moderate, 3, strong. Total score =positive percentage × intensity.

2.9 MTT cell growth assay

Transfected and control ccRCC cells (3000 cells/well) were seeded into 96-well plates, and cultured for 0 h, 24 h, 48 h, 72 h, 96 h at 37 °C with 5% CO2. The viability of cells was assessed using a CellTiter-Blue® (CTB) cell viability assay (CTB169, Promega, Beijing, China). Every 24h of testing, using 20 μl of MTT reagent to each well at different time points, cells were incubated for 2 h at 37℃. The absorbance was measured at a wavelength of 490 nm.

2.10 Cell migration assay

Cancer cells (5×10^4/well) were planted in 200μl of medium without FBS seeding on the upper chamber with Matrigel-uncoated (356224, BD Biosciences). The lower chamber was filled with 500 μl medium containing 15% FBS. After incubated for 24 h at 37°C in 5% CO2, cells were fixed with 4% paraformaldehyde and the migrated cells were stained by 0.5% crystal violet (C8470, Solarbio, china), photographed and counted under a light microscope.

2.11 In vivo mice assay

4 weeks-old BALB/c male nude mice (Vital River Laboratory Animal Technology Co., Beijing, China) were used to prepare the mouse orthotopic xenograft tumor model. Before injection of mice, Luc-SN12 shNC or Luc-SN12 shP3H4 cells (1×10^6) were re-suspended in 100μl of sterilized PBS, and later mixed with Matrigel (1:1). Cells were injected orthotopically into the subcapsular space of left kidney of nude mice and marked different groups. Mice were maintained according to rules outlined by the International Animal Welfare Recommendations and in accordance with the local institutional animal welfare guideline. Four weeks later, the primary and metastatic tumors were harvested, measured, photographed and fixed for further histopathological analysis.

4-6 weeks-old BALB/c male mice were purchased to prepare the mouse orthotopic xenograft model and the steps were the same as mentioned above. Renca cells were cultured to interfere different groups. After 15 days, tumors were harvested and the results were analyzed.

2.12 Statistics

The Cancer Genome Atlas (TCGA) database was analyzed using UALCAN to determine gene expression and correlation in 533 ccRCC and 72 normal kidney samples. GraphPad Prism software version 8.0 was used to analyze all data. Results are expressed as Means ± S.D. from at least 3 independent experiments. Student's T Test was used for comparing two groups data and one-way ANOVA followed by individual comparisons with Dunnett's test was use for

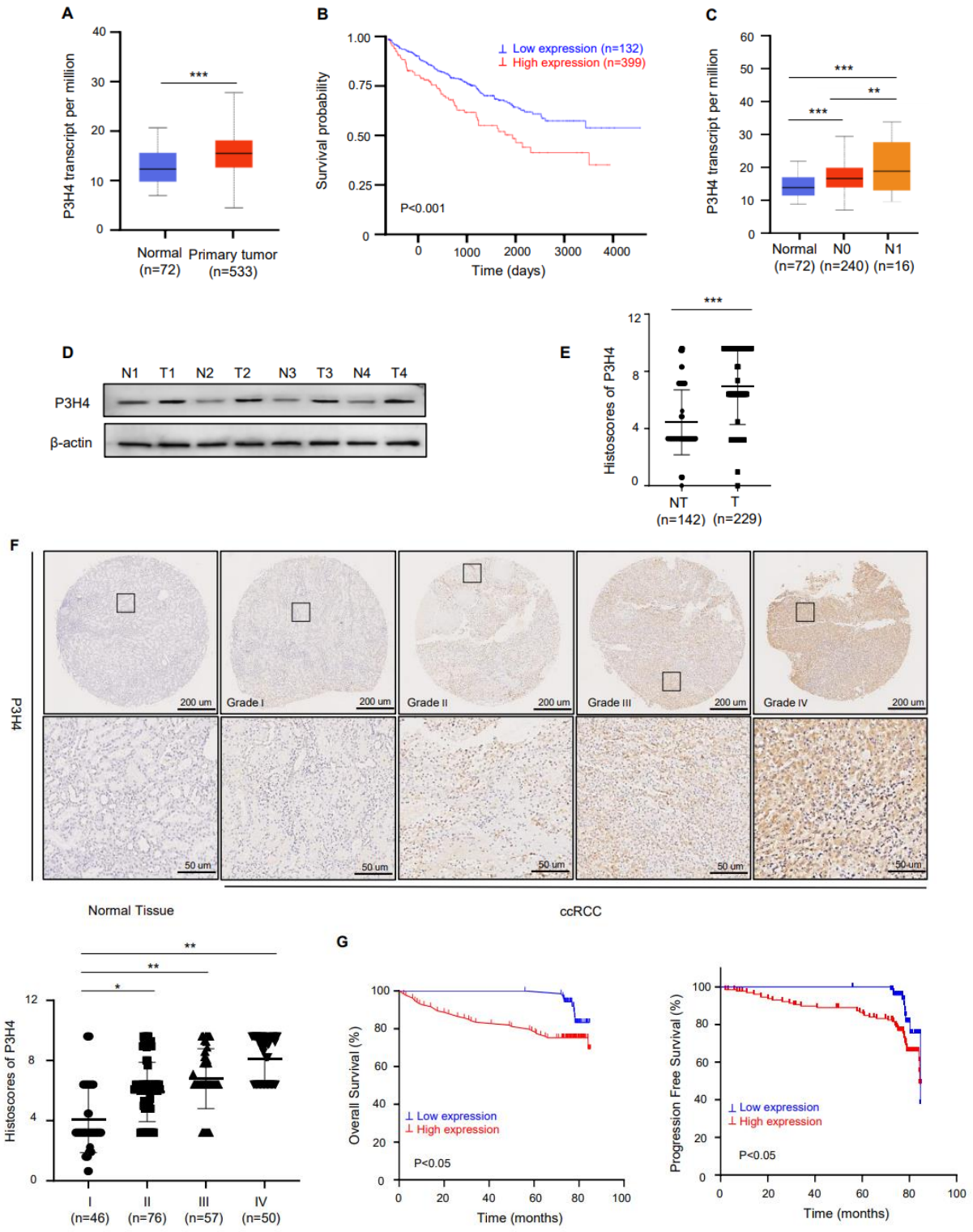

Fig. 1 High expression of P3H4 is related to the worse outcome of ccRCC patients, **A** TCGA database analyses showed the high expression of P3H4 in ccRCC tissues than that in non-tumor renal tissues, **B** Survival cures from TCGA cohort showed that ccRCC patients with high P3H4 had a short overall survival (P < 0.001), **C** High expression of P3H4 was associated with more nodal metastasis in ccRCC based on the TCGA dataset analysis, **D** Western blot analyses showed the expression of P3H4 in ccRCC and corresponding non-tumor renal tissues at protein level (n = 4), **E** Score analysis of IHC staining showed the high expression of P3H4 in ccRCC tissues (n =142) than that in non-tumor renal tissues (n =229), **F** Representative images of IHC staining demonstrated the expression level of P3H4 was associated with tumor grade in ccRCC tissues, **G** Kaplan–Meier survival analysis indicated that high expression of P3H4 was associated with poorer survival of patients with ccRCC (P<0.05), In all panels, *, P<0.05, **, P<0.01, ***, P<0.001

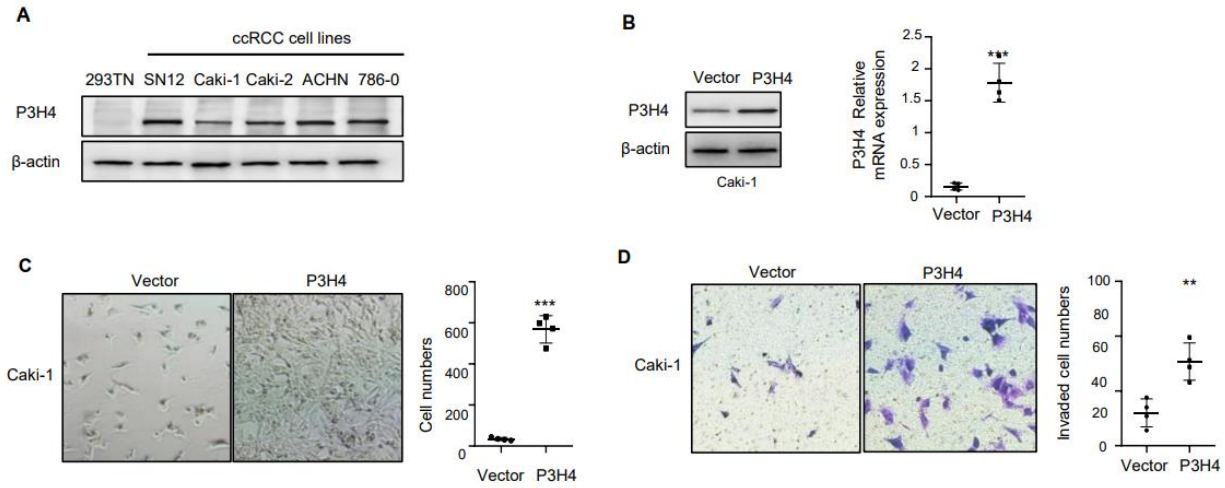

Fig. 2 P3H4 overexpression promotes cell proliferation and migration in ccRCC, A: The expression of P3H4 in one human immortalized renal epithelial cell and five ccRCC cells was analyzed by western blot analyses, B: Plasmid-mediated transfection was used to overexpress the P3H4 in Caki-1 cells, and the expression level of P3H4 was confirmed by qRT-PCR and western blot analyses, respectively, C: Cell numbers showed that overexpression of P3H4 promoted ccRCC cells growth, D: Transwell assay suggested that the migration ability of ccRCC cells was increased after overexpression of P3H4, compared to control cells. In all panels, *, P<0.05, **, P<0.01, ***, P<0.001

comparing more than two groups data. Correlations of gene expression were determined with the Pearson's coefficient test. Kaplan–Meier plots and log-rank tests were used for the overall survival analysis and progression free survival analysis. P value <0.05 was considered statistically significant.

3. Results

3.1 P3H4 is highly expressed in ccRCC and associated with worse outcome

In order to investigate the role of P3H4 in ccRCC, we analyzed the expression of P3H4 in ccRCC and normal tissues in TCGA database. The Ualcan analysis website (http://ualcan.path.uab.edu/) was used to show the P3H4 mRNA levels in 533 patients with ccRCC and 72 normal counterparts. Clinical samples analysis showed that P3H4 was highly elevated in tumors compared to normal tissues (Fig. 1A). Importantly, its high expression correlates with higher risk of distal nodal metastasis and worse overall survival (Figs. 1B and 1C). Further, western blot confirmed high expression of P3H4 in ccRCC tissues (Fig. 1D). To validate the clinical role of P3H4 in ccRCC, we performed IHC staining with anti-P3H4 antibody in renal cancer tissue samples and normal tissues. The data showed that P3H4 was significantly upregulated in tumor tissues (Fig. 1E) and high expression of P3H4 was in positively correlated with poorly differentiated grade (Fig. 1F). In addition, statistical analysis showed that expression of P3H4 in ccRCC was associated with gender, tumor diameter and Fuhrman nuclear grade (Table 1). Moreover, ccRCC patients with high expression of P3H4 had adverse overall survival and progression free survival (Fig. 1G). These results demonstrated that P3H4 was a novel risk factor for ccRCC.

3.2 Overexpression of P3H4 promotes ccRCC proliferation and migration

Since P3H4 is predominantly overexpressed in ccRCC, we sought to determine whether P3H4 plays critical role in the proliferation of renal cancer cells. We first detected the P3H4 expression in a series of renal cancer cell lines. Western blot analyses showed higher level of P3H4 in ccRCC cells than that in HEK293TN cells (Fig. 2A). Then we selected Caki-1 with relative low expression of P3H4 to transfect with plasmid containing the coding sequence of P3H4, and overexpression of it was confirmed by qRT-PCR and western blot analyses, respectively (Fig. 2B). Compared to vector-transfected cells, P3H4 overexpression significantly increased the cell numbers cultured 48 hours later in Caki-1 cell. (Fig. 2C). In addition, transwell migration assay showed that increased P3H4 could also enhance the migration ability of ccRCC cell (Fig. 2D). These evidences suggest P3H4 play an oncogenic role in ccRCC.

3.3 Inhibition of P3H4 suppresses growth and metastasis of ccRCC cells

Inversely, Caki-2 and SN12 cells with relatively high expression of P3H4 were transfected with three shRNAs targeting P3H4 and the knockdown effect was confirmed by western blot (Fig. 3A). Then, the in vitro and in vivo functional studies were performed to analyze the effect of P3H4 silencing on ccRCC cell growth and metastasis. Firstly, knockdown of P3H4 in SN12 and Caki-2 cells highly constrained cell proliferation (Fig. 3B) and cell migration (Fig. 3C). Later, flow cytometry showed that inhibition of P3H4 induced robust cell apoptosis (Fig. 3D). Meanwhile, we built two primary clear cell renal cancer cell lines from fresh tumor tissue samples and generated primary ccRCC cells stably overexpressing shP3H4 which

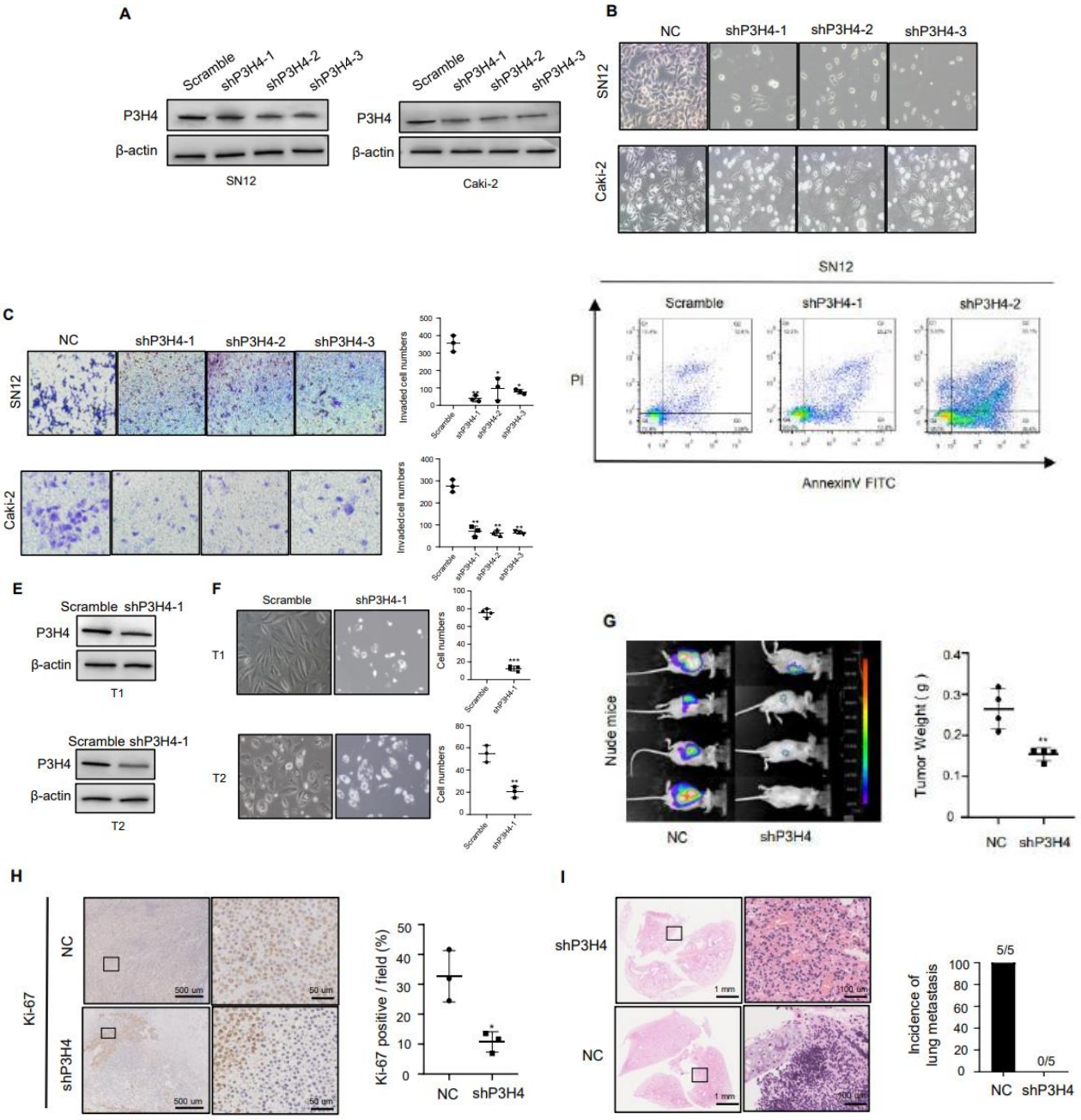

Fig. 3 Downregulation of P3H4 blocks both tumor growth and metastasis in ccRCC cells, A: Three shRNAs were used to downregulate the expression of P3H4 in SN12 and Caki-2 cells, and the knockdown of P3H4 was confirmed by western blot analyses, B: Cell numbers showed interference of P3H4 reduced ccRCC cells proliferation, C: Transwell assay showed migration ability of ccRCC cells was decreased with knockdown of P3H4, D: Apoptosis was examined by flow cytometry and results showed the percentage of cell death was increased with P3H4 knockdown, E: Primary renal cancer cells were cultivated with depletion of P3H4 and cell numbers were reduced and western blot assay tested the effect of P3H4, F: Cell numbers demonstrated constrained proliferation ability of ccRCC cells with decreased expression of P3H4, G: SN12 cells after knockdown of P3H4 were orthotopically injected into nude mice, and ex vivo bioluminescent imaging showed tumor weights were decreased (n = 4 mice per group), H: IHC staining with antibodies against Ki-67 in xenograft tumors derived from SN12 cells with P3H4 silencing, I: HE staining confirmed the lung metastasis, and the incidence of metastasis was indicated in right panel (n =5 mice per group), In all panels, *, P<0.05, **, P<0.01, ***, P<0.001

Was found to efficiently reduce P3H4 expression (Fig. 3E). In accordance with previous results, dWownregulation of P3H4 in primary ccRCC cells also significantly suppressed the proliferation and survival (Fig. 3F).

Furthermore, we performed xenograft studies in nude mice to determine the effects of P3H4 on tumorigenesis.

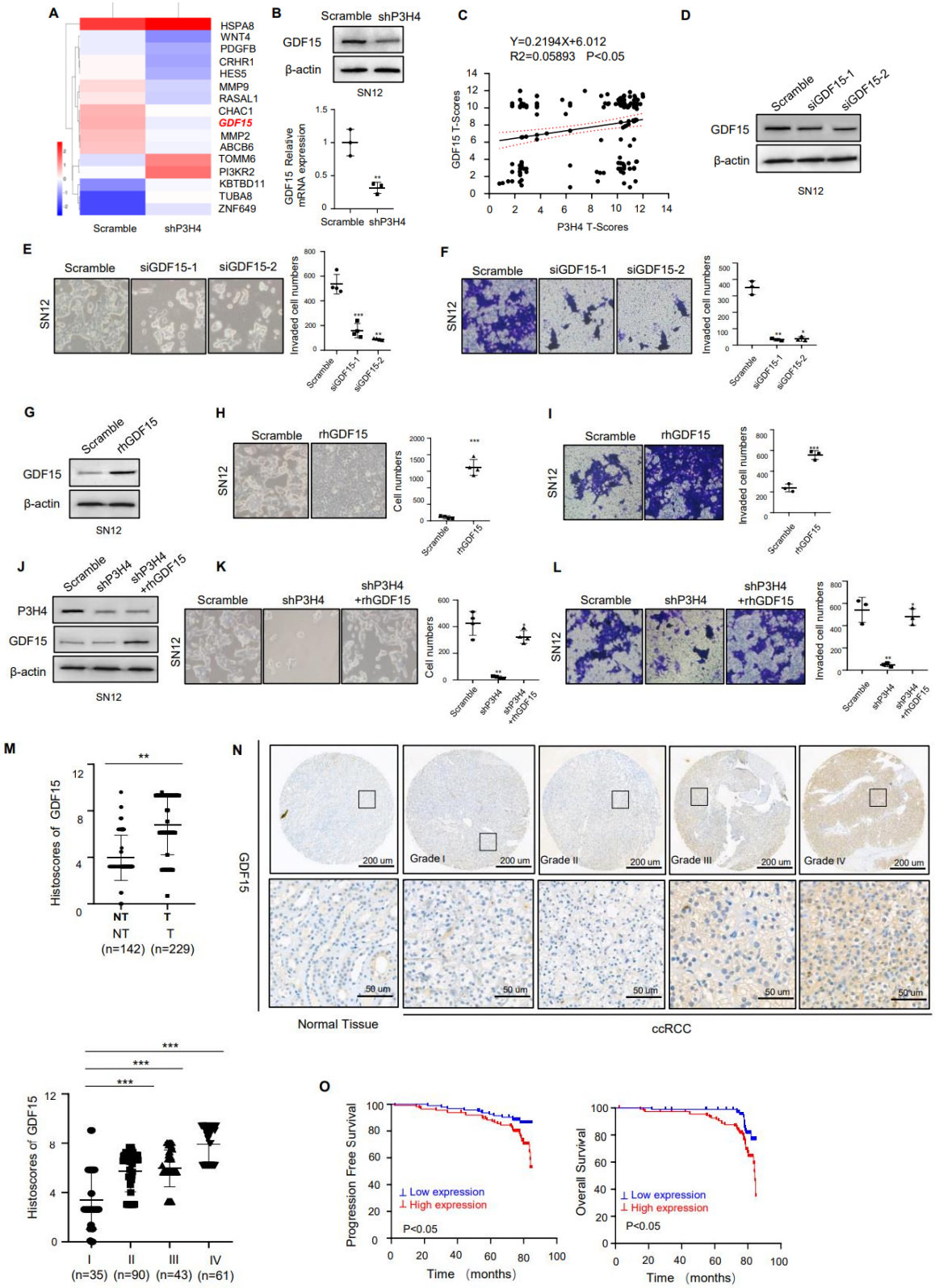

Fig. 4 P3H4 promotes ccRCC progression through stimulating GDF15 expression, A: RNA-sequencing was performed on SN12 cells transfected with or without shRNA targeting P3H4, and the genes with significant changes were indicated by heat map, B: The expression of GDF15 in SN12 cells after knockdown of P3H4 were analyzed by western blot analysis and qRT-PCR, C: IHC staining analysis in ccRCC tissue array showed the positive correlation between the expressions of P3H4 and GDF15 ($P<0.05$), D: Two siRNAs were used to downregulate the expression of GDF15 and western blot analysis showed the decreased level of GDF15 in SN12 cells, E: Cell numbers showed the cell growth activity was significantly reduced after GDF15 silencing, F Transwell assay showed silencing GDF15

reduced cell migration ability. G: Western blot analysis showed that the protein level of GDF15 was increased after treating rhGDF15 protein. H: Cell numbers showed the increased proliferation ability after treating rhGDF15 protein in SN12 cells. I: Transwell assay showed migration ability of ccRCC cells was upregulated with rhGDF15 protein. J: Levels of P3H4 and GDF15 were detected by western blot analysis after knockdown of P3H4 with or without rhGDF15 protein. K: Cell numbers showed the ability of growth was rescued by rhGDF15 protein after P3H4 knockdown. L: Transwell assay showed migration ability of ccRCC cells was upregulated with rhGDF15 protein after silencing P3H4. M: Histoscores of GDF15 showed the higher level of it in tumor patients. N: Representative images of IHC staining demonstrated the expression level of GDF15 was associated with tumor grade in ccRCC tissues. O: Survival curves based on IHC staining indicated the poorer outcome of ccRCC patients with high expression of GDF15 than those with low level of GDF15 ($P<0.05$). In all panels, *, $P<0.05$, **, $P<0.01$, ***, $P<0.001$.

SN12 cells with knockdown of P3H4 which stably expressed luciferase were orthotopically transplanted into nude mice, and the tumor weights were assessed after 4 weeks. Results showed that P3H4 knockdown dramatically decreased tumor growth (Fig. 3G). IHC staining also confirmed the decreased expression of Ki67 in P3H4 knockdown groups compared to control counterparts (Fig. 3H). Moreover, lung metastasis was detected and results indicated that inhibition of P3H4 suppressed ccRCC cell metastasis (Fig. 3I). Taken together, these data indicate P3H4 plays a vital role in ccRCC growth and metastasis.

3.4 GDF15 acts as a downstream effector of P3H4 to promote ccRCC progression

To understand the mechanisms underlying P3H4 function in ccRCC cells, we performed RNA sequencing of SN12 cells with or without P3H4 silencing and found growth differentiation factor 15 (GDF15), which plays pivotal role in regulating metabolism and tumor progression (Bucalo *et al*. 2018, Assadi *et al*. 2020), was remarkably changed (Figs. 4A and 4B). Western blot assays and qRT-PCR confirmed that P3H4 knockdown greatly downregulated GDF15, expression (Fig. 4B). Moreover, TCGA dataset and IHC staining revealed positive correlation between GDF15 and P3H4 in ccRCC tissues (Fig. 4C). Since the role of GDF15 has not been elucidated, we knockdown GDF15 with siRNAs in SN12 cells and decreased its expression (Fig. 4D). Functional analysis revealed that decreased GDF15 expression significantly inhibited renal cancer cell growth and migration (Fig. 4E and 4F). Moreover, recombinant human GDF15 (rhGDF15) could notably promote the proliferation and migration of SN12 cells (Figs. 4G-4I). Importantly, rhGDF15 could rescue the inhibition of cell growth and migration induced by P3H4 knockdown in SN12 cells (Figs. 4J-4L). Therefore, P3H4 promotes ccRCC progression via upregulation of GDF15.

Since GDF15 plays important roles in carcinogenesis (Zhang *et al*. 2019, Ahmed *et al*. 2021, Buchholz *et al*. 2021, Guo *et al*. 2021), we further explored its expression by IHC staining in ccRCC tissues. Results showed that GDF15 was highly expressed in ccRCC patients and its high expression was associated with tumor grade (Fig. 4M and 4N). Meanwhile, survival analysis indicated that ccRCC patients with high expression of GDF15 had shorter overall survival and progression free survival (Fig. 4O). In conclusion, dysregulation of P3H4-GDF15 axis enhanced ccRCC progression.

3.5 Inhibition of P3H4-GDF15 axis represses MMP9 related signaling pathway

Recent studies showed matrix metalloproteinases2/9 (MMP2/9) played important roles in tumor invasion which could be regulated by GDF15 (Griner *et al*. 2013), and revealed its oncogenic function in ccRCC (Ma *et al*. 2012, Qian *et al*. 2018, Lee *et al*. 2019). RNA-sequencing and western blot assays revealed the downregulation of MMP2/9 in SN12 cells with knockdown of P3H4 (Figs. 5A and 5B), which indicated the underlying role of MMPs in P3H4-GDF15 axis. Previous studies showed the regulation of MMPs by GDF15 mainly through EMT pathway and Ras/Erk pathway in tumor tissues (Abd El-Aziz *et al*. 2007, Griner *et al*. 2013). Surprisingly, western blot assays suggested the depletion of P3H4 or GDF15 could inhibit EMT process and Ras signal activation. (Fig. 5C and 5D). Meanwhile, overexpression of GDF15 after knockdown of P3H4 could upregulate the expression of MMP2/9 and its related pathway molecules in SN12 cells (Fig. 5E). These results showed MMP2/9 participate in the role of P3H4-GDF15 axis in ccRCC.

Furthermore, TCGA database and IHC staining revealed a positive correlation between GDF15 and MMP9 levels in renal cancer (Figs. 5A and 5F), and histoscores showed the high level of MMP9 in tumor tissues (Fig. 5G). Survival analysis suggested high expression of MMP9 was associated with the worse outcome of patients with ccRCC (Fig. 5H). IHC staining analyses showed the co-expression of P3H4 and MMP9 in ccRCC tissues had shorter prognosis (Fig. 5I). The TCGA database also showed the positive correlationship among P3H4, GDF15 and MMP9 (Fig. 5B) and ccRCC patients with high level of P3H4/GDF15/MMP9 had the worst outcome (Fig. 5C). Therefore, P3H4/GDF15/MMP9 axis was a promising prognostic factor for patients with ccRCC.

3.6 P3H4 facilitates tumor-mediated immune-suppression via regulating MMP9/PD-L1 axis

MMP2/9 inhibitor was reported to diminish both mRNA and protein levels of PD-L1 (Wei *et al*. 2018, Zhao *et al*. 2018), and combination of MMP9 inhibitor and anti-PD1 antibody to treat cancer had shown good prospects (Imai and Takaoka 2006, Zhu and Li 2018, Smith *et al*. 2019, Ye *et al*. 2020). Western blot and qRT-PCR showed that P3H4 silencing decreased PD-L1 expression in 786-O cells (Figs. 6A and 6B). Besides, the downregulation of GDF15 using

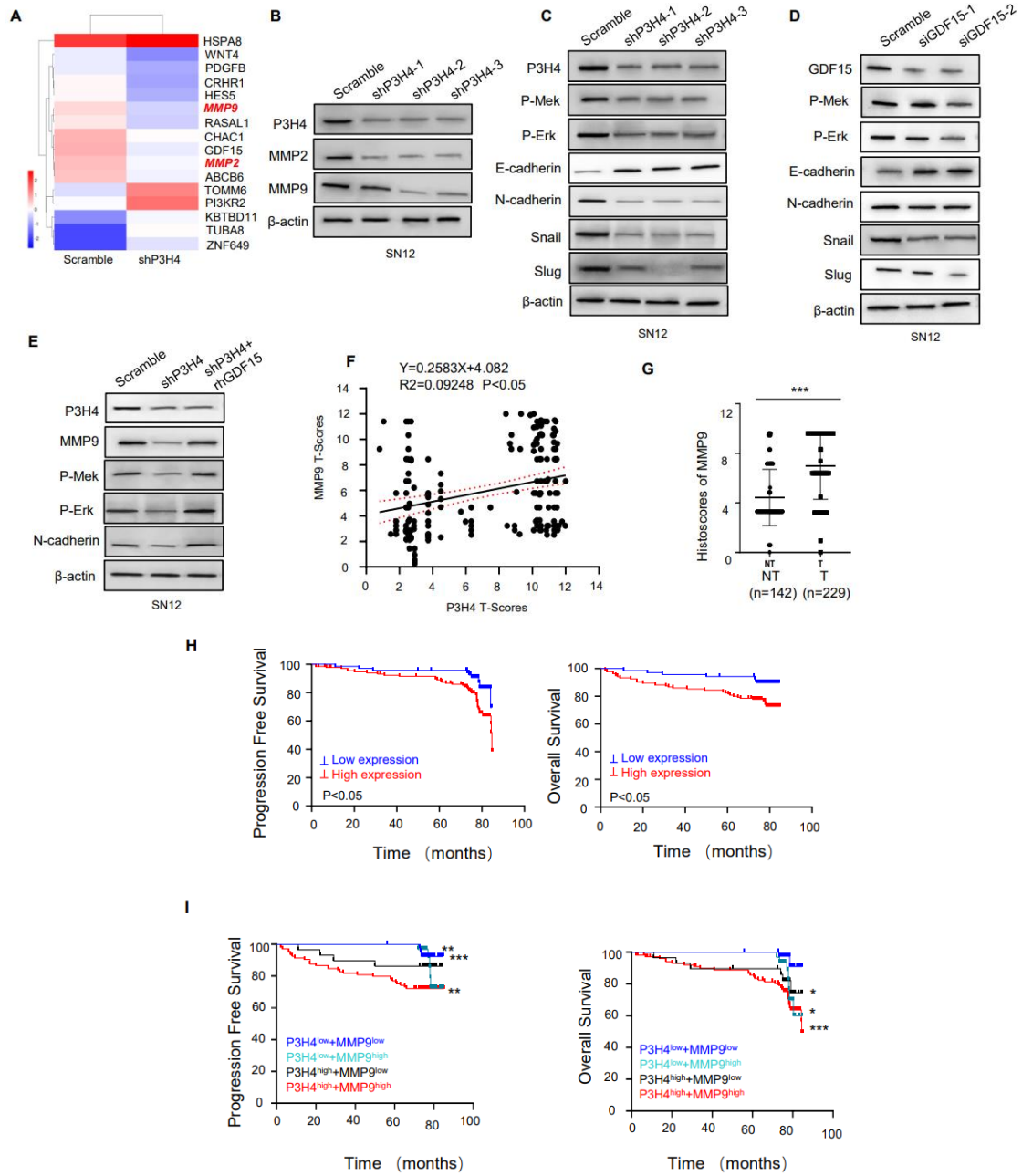

Fig. 5 Positive regulation of MMP9 related signaling pathway through P3H4-GDF15 axis in ccRCC, A: RNA-sequencing was performed in SN12 cells with P3H4 silencing, and heat map showed the decreased levels of MMP2/9 after knockdown of P3H4, B: Western blot assays showed the expression of MMP2/9 in SN12 cells with P3H4 knockdown, C: Western blot assays showed the downregulation of EMT pathway and Ras/Erk pathway with decreased level of P3H4, D: Western blot illustrated the inactivated EMT pathway and Ras/ERK pathway after knockdown GDF15 in SN12 cells, E: Western blot showed rhGDF15 protein rescued the level of EMT pathway and Ras pathway induced by P3H4 knockdown, F: IHC staining analysis in ccRCC tissue array showed the positive correlation between the expressions of P3H4 and MMP9 ($P<0.05$), G: IHC staining analysis showed the high expression of MMP9 in ccRCC tissues, H: Survival analysis showed worse outcome of patients with upregulation of MMP9 based on IHC staining, I: Survival analysis suggested high expression of both P3H4 and MMP9 in ccRCC patients had shorter outcome than other groups. In all panels, *, $P<0.05$, **, $P<0.01$, ***, $P<0.001$.

siRNA in 786-O cells also suppressed the expression of PD-L1 (Fig. 6C). Moreover, rhMMP9 protein rescued the decreased expression of PD-L1 caused by knockdown of P3H4 (Fig. 6D). These results suggested the potential role of P3H4/GDF15/MMP9 axis in immunosuppression via upregulating the expression of PD-L1.

To investigate the role of P3H4 in modulation of tumor microenvironment, m-shP3H4 plasmid sequences were transfected into renca cells, and the knockdown effect was confirmed by western blot and qRT-PCR (Figs. 6E and 6F).

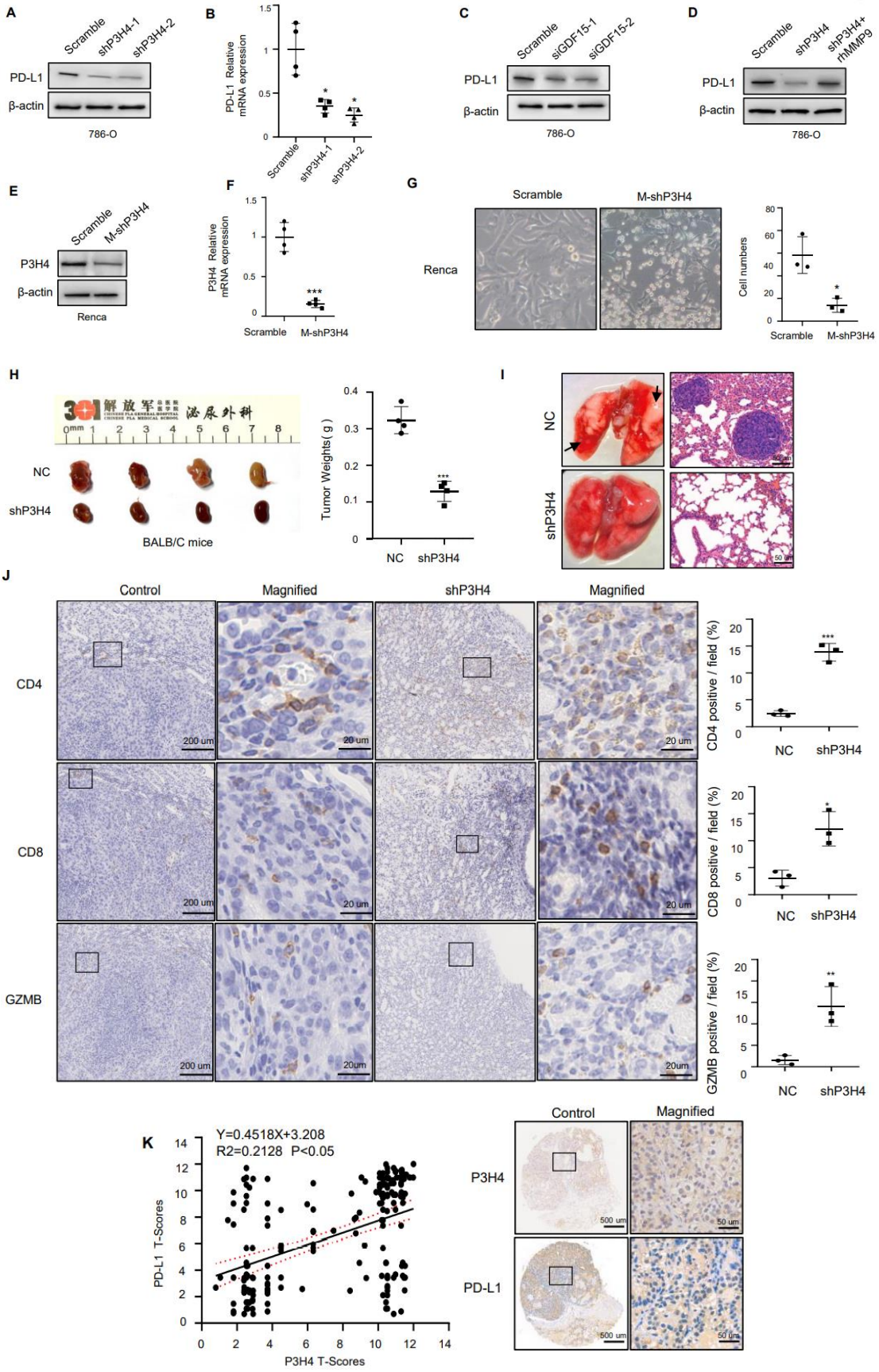

Fig. 6 P3H4 regulates tumor-associated immunosuppression by activating MMP9-PD-L1 axis. A, B: Western blot analysis and qRT-PCR showed the decreased expression of PD-L1 in 786-O cells after P3H4 knockdown, respectively. C: Western blot analysis illustrated the decreased level of PD-L1 in 786-O cells with GDF15 silencing. D: Western blot analysis showed the upregulation of PD-L1 after P3H4 silencing with rhMMP9 compared to cells

with knockdown of P3H4 in 786-O cells. E-F: Western blot analysis and qRT-PCR showed the down-regulation of P3H4 in renca cells with knockdown of P3H4. G: Cell numbers showed the decreased ability of proliferation in renca cells with P3H4 silencing. H: Renca cells with P3H4 silencing were orthotopically injected into BALB/C mice, and the tumor weights were measured after 18 days (n = 4 mice per group). I: HE staining showed decreased metastasis after knockdown of P3H4 in BLBL/C mice. J: IHC staining showed the increased infiltration of CD4+/CD8+/GZMB after knockdown of P3H4 in mice. K: IHC staining analysis in ccRCC tissue array showed the positive correlation between the expressions of P3H4 and PD-L1 (P<0.05). In all panels, *, P<0.05, **, P<0.01, ***, P<0.001.

MTT assays showed that inhibition of P3H4 constrained the proliferation of renca cells (Fig. 6G). Later, we orthotopically transplanted renca cells with or without P3H4 interference into BALB/c mice. The weight of tumors were assessed after 18 days, and results showed smaller of tumor tissues in shP3H4 groups compared to control groups (Fig. 6H). HE staining of Lung tissues revealed that downregulation of P3H4 dramatically repressed metastasis ability of renal cancer cells (Fig. 6I). Furthermore, we conducted IHC staining and results showed that both the intratumor infiltration of $CD4^+$ and $CD8^+$ T cells and cytotoxic activity marked by granzyme B were remarkably increased in shP3H4 groups (Fig. 6J), indicating that P3H4 deprivation triggers robust anti-tumor immunity. Meanwhile, we also found a positive correlation between P3H4 expression and PD-L1 level in clinical specimens (Fig. 6K). The tissue samples of TCGA database showed the positive relationship between P3H4 and infiltration of $CD4^+$ and $CD8^+$ T cells (Supplementary Figs. 6A and 6B). Taken together, these results for the first time showed the novel role of P3H4 in tumor-mediated immunosuppression.

4. Discussion

Although it has provided that P3H4 gene could behave as oncogene in cancer progression (Hao *et al*. 2020), the function of P3H4 in ccRCC is largely unknown. In this study, we firstly proved that the expression of P3H4 was aberrantly increased in ccRCC, which promoted cell proliferation and metastasis in vitro and in vivo, and predicted the worse survival of patients with ccRCC. Furthermore, functional studies showed that GDF15 and MMPs, which were regulated by P3H4, participated in the progression of ccRCC. Moreover, we demonstrated that inhibition of P3H4-GDF15-MMP9 axis could suppress the immune system to constrain tumor progression by decreasing PD-L1 protein levels, suggesting that manipulating the inhibitor of P3H4-GDF15-MMP9 axis may synergize with the immune checkpoint blockade therapy in ccRCC patients.

Notably, our study revealed GDF15 worked as the downstream of P3H4 in tumor progression and knockdown of P3H4 significantly decreased mRNA and protein levels of GDF15, thus, it will be interesting to find out how P3H4 regulates GDF15 in ccRCC. P3H4 usually services as posttranslational modification (Hudson and Eyre 2013) and we guest that it may participate in regulating the regulator of GDF15 during transcription and translation. Moreover, we firstly explored the function of GDF15 in ccRCC and found its oncogenic role in promoting cancer cells proliferation and migration.

Recent studies also reported that GDF15 acts on immune cells and promotes cancer by mediating immune escape in the tumor microenvironment (Lodi *et al*. 2021), and our results showed that constrained level of GDF15 highly decreased expression of PD-L1, providing a novel mechanism for GDF15 in immunosuppression. Meanwhile, as a metabolic signature for cachexia in patients with cancer (Lerner *et al*. 2015), it will also be interesting to uncover the metabolic role of GDF15 in ccRCC and explore its clinical potential as therapeutic target.

Particularly, MMP9 inhibitor modulated tumor immune surveillance by regulating PD-L1 and the combination of MMP inhibitors and anti-PD-1 was used to treat gastric and esophageal cancers in the phase III clinical trial (64). We found that rhMMP9 could rescued the downregulation of PD-L1 caused by knockdown of P3H4 or GDF15 in ccRCC, and these evidences suggested the role of MMP9 in immunosuppression in ccRCC. Also, it's worthy to clarify whether the combination of MMP9 inhibitors and anti-PD-1 drugs can treat patients with ccRCC. Later, it's interesting to study that the efficiency of GDF15 inhibitor in ccRCC and the combination of immunotherapy.

5. Conclusions

Our study detailedly investigates the expression levels, clinical significances, and functions of P3H4 and its downstream effector GDF15 in ccRCC, and identifies a novel P3H4-GDF15-MMP9 axis in tumor-mediated immunosuppression via regulating PD-L1, providing potential targets for the prognosis and treatment of patients with ccRCC.

Acknowledgements

This work was supported by National Natural Science Foundation of China (Grand No. 81972389 and 81770790), and Distinguished Young Scholar Project of PLA General Hospital (Grand No. 2020-JQPY-002).

References

Abd El-Aziz, S.H., Endo, Y., Miyamaori, H., Takino, T. and Sato, H. (2007), "Cleavage of growth differentiation factor 15 (GDF15) by membrane type 1-matrix metalloproteinase abrogates GDF15-mediated suppression of tumor cell growth", *Cancer Sci*., **98**(9), 1330-1335. https://doi.org/10.1111/j.1349-7006.2007.00547.x.

Ahmed, D.S., Isnard, S., Lin, J., Routy, B. and Routy, J.P. (2021), "GDF15/GFRAL pathway as a metabolic signature for cachexia in patients with cancer", *J. Cancer*., **12**(4), 1125-1132.

https://doi.org/10.7150/jca.50376.
Assadi, A., Zahabi, A. and Hart, R.A. (2020), "GDF15, an update of the physiological and pathological roles it plays: A review", *Pflug. Arch. Eur. J. Phys.*, **472**(11), 1535-1546. https://doi.org/10.1007/s00424-020-02459-1.
Baek, S.J. and Eling, T. (2019), "Growth differentiation factor 15 (GDF15): A survival protein with therapeutic potential in metabolic diseases", *Pharmacol. Ther.*, **198**, 46-58. https://doi.org/10.1016/j.pharmthera.2019.02.008.
Bucalo, M.L., Barbieri, C., Roca, S., Ion Titapiccolo, J., Ros Romero, M.S., Ramos, R., Albaladejo, M., Manzano, D., Mari, F. and Molina, M. (2018), "The anaemia control model: Does it help nephrologists in therapeutic decision-making in the management of anaemia?", *Nefrología*, **38**(5), 491-502. https://doi.org/10.1016/j.nefroe.2018.10.001.
Buchholz, K., Antosik, P., Grzanka, D., Gagat, M., Smolinska, M., Grzanka, A., Gzil, A., Kasperska, A. and Klimaszewska-Wisniewska, A. (2021), "Expression of the body-weight signaling players: GDF15, GFRAL and RET and their clinical relevance in gastric cancer", *J. Cancer*, **12**(15), 4698-4709. https://doi.org/10.7150/jca.55511.
Chen, Q., Pearlman, R.E. and Moens, P.B. (1992), "Isolation and characterization of a cDNA encoding a synaptonemal complex protein", *Biochem. Cell Biol.*, **70**(10-11), 1030-1038. https://doi.org/10.1139/o92-147.
Coll, A.P., Chen, M., Taskar, P., Rimmington, D., Patel, S., Tadross, J.A., Cimino, I., Yang, M., Welsh, P., Virtue, S., Goldspink, D.A., Miedzybrodzka, E.L., Konopka, A.R., Esponda, R.R., Huang, J.T., Tung, Y.C.L., Rodriguez-Cuenca, S., Tomaz, R.A., Harding, H.P., Melvin, A., Yeo, G.S.H., Preiss, D., Vidal-Puig, A., Vallier, L., Nair, K.S., Wareham, N.J., Ron, D., Gribble, F.M., Reimann, F., Sattar, N., Savage, D.B., Allan, B.B. and O'Rahilly, S. (2020), "GDF15 mediates the effects of metformin on body weight and energy balance", *Nature*, **578**(7795), 444-448. https://doi.org/10.1038/s41586-019-1911-y.
Coussens, L.M., Fingleton, B. and Matrisian, L.M. (2002), "Matrix metalloproteinase inhibitors and cancer: trials and tribulations", *Science*, **295**(5564), 2387-2392. https://doi.org/10.1126/science.1067100.
Day, E.A., Ford, R.J., Smith, B.K., Mohammadi-Shemirani, P., Morrow, M.R., Gutgesell, R.M., Lu, R., Raphenya, A.R., Kabiri, M., McArthur, A.G., McInnes, N., Hess, S., Pare, G., Gerstein, H.C. and Steinberg, G.R. (2019), "Metformin-induced increases in GDF15 are important for suppressing appetite and promoting weight loss", *Nat. Metab.*, **1**(12), 1202-1208. https://doi.org/10.1038/s42255-019-0146-4.
Dorandish, S., Williams, A., Atali, S., Sendo, S., Price, D., Thompson, C., Guthrie, J., Heyl, D. and Evans, H.G. (2021), "Regulation of amyloid-beta levels by matrix metalloproteinase-2/9 (MMP2/9) in the media of lung cancer cells", *Sci. Rep.*, **11**(1), 9708. https://doi.org/10.1038/s41598-021-88574-0.
Du, W., Zhang, L., Brett-Morris, A., Aguila, B., Kerner, J., Hoppel, C.L., Puchowicz, M., Serra, D., Herrero, L., Rini, B.I., Campbell, S. and Welford, S.M. (2017), "HIF drives lipid deposition and cancer in ccRCC via repression of fatty acid metabolism", *Nat. Commun.*, **8**(1), 1769. https://doi.org/10.1038/s41467-017-01965-8.
Egeblad, M. and Werb, Z. (2002), "New functions for the matrix metalloproteinases in cancer progression", *Nat. Rev. Cancer.*, **2**(3), 161-174. https://doi.org/10.1038/nrc745.
Escudier, B., Porta, C., Schmidinger, M., Rioux-Leclercq, N., Bex, A., Khoo, V., Grunwald, V., Gillessen, S. and Horwich, A. (2019), "Renal cell carcinoma: ESMO Clinical Practice Guidelines for diagnosis, treatment and follow-updagger", *Ann. Oncol.*, **30**(5), 706-720. https://doi.org/10.1093/annonc/mdz056.
Fields, G.B. (1991), "A model for interstitial collagen catabolism by mammalian collagenases", *J. Theor. Biol.*, **153**(4), 585-602. https://doi.org/10.1016/s0022-5193(05)80157-2.
Fields, G.B. (2013), "Interstitial collagen catabolism", *J. Biol. Chem.*, **288**(13), 8785-8793. https://doi.org/10.1074/jbc.R113.451211.
Griner, S.E., Joshi, J.P. and Nahta, R. (2013), "Growth differentiation factor 15 stimulates rapamycin-sensitive ovarian cancer cell growth and invasion", *Biochem. Pharmacol.*, **85**(1), 46-58. https://doi.org/10.1016/j.bcp.2012.10.007.
Gruenwald, K., Castagnola, P., Besio, R., Dimori, M., Chen, Y., Akel, N.S., Swain, F.L., Skinner, R.A., Eyre, D.R., Gaddy, D., Suva, L.J. and Morello, R. (2014), "Sc65 is a novel endoplasmic reticulum protein that regulates bone mass homeostasis", *J. Bone Miner. Res.*, **29**(3), 666-675. https://doi.org/10.1002/jbmr.2075.
Guo, F., Zhou, Y., Guo, H., Ren, D., Jin, X. and Wu, H. (2021), "NR5A2 transcriptional activation by BRD4 promotes pancreatic cancer progression by upregulating GDF15", *Cell Death Discov.*, **7**(1), 78. https://doi.org/10.1038/s41420-021-00462-8.
Hao, L., Pang, K., Pang, H., Zhang, J., Zhang, Z., He, H., Zhou, R., Shi, Z. and Han, C. (2020), "Knockdown of P3H4 inhibits proliferation and invasion of bladder cancer", *Aging*, **12**(3), 2156-2168. https://doi.org/10.18632/aging.102732.
Huang, L.L., Wang, Z., Cao, C.J., Ke, Z.F., Wang, F., Wang, R., Luo, C.Q., Lu, X. and Wang, L.T. (2017), "AEG-1 associates with metastasis in papillary thyroid cancer through upregulation of MMP2/9", *Int. J. Oncol.*, **51**(3), 812-822. https://doi.org/10.3892/ijo.2017.4074.
Hudson, D.M. and Eyre, D.R. (2013), "Collagen prolyl 3-hydroxylation: A major role for a minor post-translational modification?", *Connect. Tissue Res.*, **54**(4-5), 245-251. https://doi.org/10.3109/03008207.2013.800867.
Imai, K. and Takaoka, A. (2006), "Comparing antibody and small-molecule therapies for cancer", *Nat. Rev. Cancer.*, **6**(9), 714-727. https://doi.org/10.1038/nrc1913.
Jin, X., Zhou, H., Song, J., Cui, H., Luo, Y. and Jiang, H. (2021), "P3H4 overexpression serves as a prognostic factor in lung adenocarcinoma", *Comput. Math. Methods Med.*, **2021**, 9971353. https://doi.org/10.1155/2021/9971353.
Jonasch, E., Walker, C.L. and Rathmell, W.K. (2021), "Clear cell renal cell carcinoma ontogeny and mechanisms of lethality", *Nat. Rev. Nephrol.*, **17**(4), 245-261. https://doi.org/10.1038/s41581-020-00359-2.
Kessenbrock, K., Plaks, V. and Werb, Z. (2010), "Matrix metalloproteinases: Regulators of the tumor microenvironment", *Cell*, **141**(1), 52-67. https://doi.org/10.1016/j.cell.2010.03.015.
Lai, Y., Tang, F., Huang, Y., He, C., Chen, C., Zhao, J., Wu, W. and He, Z. (2021), "The tumour microenvironment and metabolism in renal cell carcinoma targeted or immune therapy", *J. Cell Physiol.*, **236**(3), 1616-1627. https://doi.org/10.1002/jcp.29969.
Lee, H.J., Cho, H.E. and Park, H.J. (2021), "Germinated black soybean fermented with Lactobacillus pentosus SC65 alleviates DNFB-induced delayed-type hypersensitivity in C57BL/6N mice", *J. Ethnopharmacol.*, **265**, 113236. https://doi.org/10.1016/j.jep.2020.113236.
Lee, Y.M., Kim, J.M., Lee, H.J., Seong, I.O. and Kim, K.H. (2019), "Immunohistochemical expression of CD44, matrix metalloproteinase2 and matrix metalloproteinase9 in renal cell carcinomas", *Urol. Oncol.*, **37**(10), 742-748. https://doi.org/10.1016/j.urolonc.2019.04.017.
Lerner, L., Hayes, T.G., Tao, N., Krieger, B., Feng, B., Wu, Z., Nicoletti, R., Chiu, M.I., Gyuris, J. and Garcia, J.M. (2015), "Plasma growth differentiation factor 15 is associated with weight loss and mortality in cancer patients", *J. Cachexia Sarcopenia Muscle*, **6**(4), 317-324. https://doi.org/10.1002/jcsm.12033.
Lerner, L., Tao, J., Liu, Q., Nicoletti, R., Feng, B., Krieger, B.,

Mazsa, E., Siddiquee, Z., Wang, R., Huang, L., Shen, L., Lin, J., Vigano, A., Chiu, M.I., Weng, Z., Winston, W., Weiler, S. and Gyuris, J. (2016), "MAP3K11/GDF15 axis is a critical driver of cancer cachexia", *J. Cachexia Sarcopenia Muscle*, **7**(4), 467-482. https://doi.org/10.1002/jcsm.12077.

Li, C., Wang, J., Kong, J., Tang, J., Wu, Y., Xu, E., Zhang, H. and Lai, M. (2016), "GDF15 promotes EMT and metastasis in colorectal cancer", *Oncotarget*, **7**(1), 860-872. https://doi.org/10.18632/oncotarget.6205.

Li, L., Zhang, R., Yang, H., Zhang, D., Liu, J., Li, J. and Guo, B. (2020), "GDF15 knockdown suppresses cervical cancer cell migration in vitro through the TGF-beta/Smad2/3/Snail1 pathway", *FEBS Open Bio*, **10**(12), 2750-2760. https://doi.org/10.1002/2211-5463.13013.

Li, S., Ma, Y.M., Zheng, P.S. and Zhang, P. (2018a), "GDF15 promotes the proliferation of cervical cancer cells by phosphorylating AKT1 and Erk1/2 through the receptor ErbB2", *J. Exp. Clin. Cancer Res.*, **37**(1), 80. https://doi.org/10.1186/s13046-018-0744-0.

Li, W., Ye, L., Chen, Y. and Chen, P. (2018b), "P3H4 is correlated with clinicopathological features and prognosis in bladder cancer", *World J. Surg. Oncol.*, **16**(1), 206. https://doi.org/10.1186/s12957-018-1507-2.

Lodi, R.S., Yu, B., Xia, L. and Liu, F. (2021), "Roles and Regulation of Growth differentiation factor-15 in the Immune and tumor microenvironment", *Hum. Immunol.*, **82**(12), 937-944. https://doi.org/10.1016/j.humimm.2021.06.007.

Lu, X., He, X., Su, J., Wang, J., Liu, X., Xu, K., De, W., Zhang, E., Guo, R. and Shi, Y.E. (2018), "EZH2-mediated epigenetic suppression of gdf15 predicts a poor prognosis and regulates cell proliferation in non-small-cell lung cancer", *Mol. Ther. Nucleic. Acids.*, **12**, 309-318. https://doi.org/10.1016/j.omtn.2018.05.016.

Ma, J.J., Kong, L.M., Liao, C.G., Jiang, X., Wang, Y. and Bao, T.Y. (2012), "Suppression of MMP-9 activity by NDRG2 expression inhibits clear cell renal cell carcinoma invasion", *Med Oncol.* **29**(5), 3306-3313. https://doi.org/10.1007/s12032-012-0265-1.

Marshall, D.C., Lyman, S.K., McCauley, S., Kovalenko, M., Spangler, R., Liu, C., Lee, M., O'Sullivan, C., Barry-Hamilton, V., Ghermazien, H., Mikels-Vigdal, A., Garcia, C.A., Jorgensen, B., Velayo, A.C., Wang, R., Adamkewicz, J.I. and Smith, V. (2015), "Selective allosteric inhibition of mmp9 is efficacious in preclinical models of ulcerative colitis and colorectal cancer", *PLoS One*, **10**(5), e0127063. https://doi.org/10.1371/journal.pone.0127063.

Motzer, R.J., Jonasch, E., Agarwal, N., Bhayani, S., Bro, W.P., Chang, S.S., Choueiri, T.K., Costello, B.A., Derweesh, I.H., Fishman, M., Gallagher, T.H., Gore, J.L., Hancock, S.L., Harrison, M.R., Kim, W., Kyriakopoulos, C., LaGrange, C., Lam, E.T., Lau, C., Michaelson, M.D., Olencki, T., Pierorazio, P.M., Plimack, E.R., Redman, B.G., Shuch, B., Somer, B., Sonpavde, G., Sosman, J., Dwyer, M. and Kumar, R. (2017), "Kidney cancer, version 2.2017, NCCN clinical practice guidelines in oncology", *J. Natl. Compr. Cancer Netw.*, **15**(6), 804-834. https://doi.org/10.6004/jnccn.2017.0100.

Nakayasu, E.S., Syed, F., Tersey, S.A., Gritsenko, M.A., Mitchell, H.D., Chan, C.Y., Dirice, E., Turatsinze, J.V., Cui, Y., Kulkarni, R.N., Eizirik, D.L., Qian, W.J., Webb-Robertson, B.M., Evans-Molina, C., Mirmira, R.G. and Metz, T.O. (2020), "Comprehensive proteomics analysis of stressed human islets identifies GDF15 as a target for type 1 diabetes intervention", *Cell. Metab.* **31**(2), 363-374 e366. https://doi.org/10.1016/j.cmet.2019.12.005.

Ochs, R.L., Stein Jr, T.W., Chan, E.K., Ruutu, M. and Tan, E.M. (2017), "cDNA cloning and characterization of a novel nucleolar protein", *Mol. Biol. Cell.*, **7**(7), 1015-1024. https://doi.org/10.1091/mbc.7.7.1015.

Qian, H., Li, X., Zhang, W., Ma, L., Sun, J., Tang, X., Chen, Y., Teng, L., Wang, W., Li, D., Xu, Y., Li, C. and Cao, Y. (2018), "Caspase-10, matrix metalloproteinase-9 and total laminin are correlated with the tumor malignancy of clear cell renal cell carcinoma", *Oncol. Lett.*, **16**(2), 2039-2045. https://doi.org/10.3892/ol.2018.8845.

Roy, R., Yang, J. and Moses, M.A. (2009), "Matrix metalloproteinases as novel biomarkers and potential therapeutic targets in human cancer", *J. Clin. Oncol.*, **27**(31), 5287-5297. https://doi.org/10.1200/JCO.2009.23.5556.

Smith, W.M., Purvis, I.J., Bomstad, C.N., Labak, C.M., Velpula, K.K., Tsung, A.J., Regan, J.N., Venkataraman, S., Vibhakar, R. and Asuthkar, S. (2019), "Therapeutic targeting of immune checkpoints with small molecule inhibitors", *Am. J. Transl. Res.*, **11**(2), 529-541.

Spanopoulou, A. and Gkretsi, V. (2020), "Growth differentiation factor 15 (GDF15) in cancer cell metastasis: from the cells to the patients", *Clin. Exp. Metastas.*, **37**(4), 451-464. https://doi.org/10.1007/s10585-020-10041-3.

Suriben, R., Chen, M., Higbee, J., Oeffinger, J., Ventura, R., Li, B., Mondal, K., Gao, Z., Ayupova, D., Taskar, P., Li, D., Starck, S.R., Chen, H.H., McEntee, M., Katewa, S.D., Phung, V., Wang, M., Kekatpure, A., Lakshminarasimhan, D., White, A., Olland, A., Haldankar, R., Solloway, M.J., Hsu, J.Y., Wang, Y., Tang, J., Lindhout, D.A. and Allan, B.B. (2020), "Antibody-mediated inhibition of GDF15-GFRAL activity reverses cancer cachexia in mice", *Nat Med.* **26**(8), 1264-1270. https://doi.org/10.1038/s41591-020-0945-x.

Tsai, V.W.W., Husaini, Y., Sainsbury, A., Brown, D.A. and Breit, S.N. (2018), "The MIC-1/GDF15-GFRAL pathway in energy homeostasis: Implications for obesity, cachexia, and other associated diseases", *Cell. Metab.*, **28**(3), 353-368. https://doi.org/10.1016/j.cmet.2018.07.018.

Van Doren, S.R. (2015), "Matrix metalloproteinase interactions with collagen and elastin", *Matrix Biol.*, **44-46**, 224-231. https://doi.org/10.1016/j.matbio.2015.01.005.

Wan, B., Zeng, Q., Tang, X.Z. and Tang, Y.X. (2018), "P3H4 affects renal carcinoma through up-regulating miR-1/133a", *Eur. Rev. Med. Pharmacol. Sci.*, **22**(16), 5180-5186. https://doi.org/10.26355/eurrev_201808_15714.

Wei, M., Liu, X., Cao, C., Yang, J., Lv, Y., Huang, J., Wang, Y. and Qin, Y. (2018), "An engineered PD-1-based and MMP-2/9-oriented fusion protein exerts potent antitumor effects against melanoma", *BMB Rep.*, **51**(11), 572-577. https://doi.org/10.5483/BMBRep.2018.51.11.076.

Weliky, N., Leaman, D.H., Jr. and Kallman, B.J. (1975), "Stability and dissociation of P3H4-1 Burkitt's lymphoma cell soluble complement-fixing antigen identified with human serum", *Cancer Res.* **35**(6), 1580-1585.

Yang, C., Yu, H., Chen, R., Tao, K., Jian, L., Peng, M., Li, X., Liu, M. and Liu, S. (2019), "CXCL1 stimulates migration and invasion in ERnegative breast cancer cells via activation of the ERK/MMP2/9 signaling axis", *Int. J. Oncol.*, **55**(3), 684-696. https://doi.org/10.3892/ijo.2019.4840.

Ye, Y., Kuang, X., Xie, Z., Liang, L., Zhang, Z., Zhang, Y., Ma, F., Gao, Q., Chang, R., Lee, H.H., Zhao, S., Su, J., Li, H., Peng, J., Chen, H., Yin, M., Peng, C., Yang, N., Wang, J., Liu, J., Liu, H., Han, L. and Chen, X. (2020), "Small-molecule MMP2/MMP9 inhibitor SB-3CT modulates tumor immune surveillance by regulating PD-L1", *Genome Med.* **12**(1), 83. https://doi.org/10.1186/s13073-020-00780-z.

Yue, Y.C., Yang, B.Y., Lu, J., Zhang, S.W., Liu, L., Nassar, K., Xu, X.X., Pang, X.Y. and Lv, J.P. (2020), "Metabolite secretions of Lactobacillus plantarum YYC-3 may inhibit colon cancer cell metastasis by suppressing the VEGF-MMP2/9 signaling pathway", *Microb. Cell Fact.*, **19**(1), 213.

https://doi.org/10.1186/s12934-020-01466-2.
Zhang, W., Hu, C., Wang, X., Bai, S., Cao, S., Kobelski, M., Lambert, J.R., Gu, J. and Zhan, Y. (2019), "Role of GDF15 in methylseleninic acid-mediated inhibition of cell proliferation and induction of apoptosis in prostate cancer cells", *PLoS One*, **14**(9), e0222812. https://doi.org/10.1371/journal.pone.0222812.
Zhao, F., Evans, K., Xiao, C., DeVito, N., Theivanthiran, B., Holtzhausen, A., Siska, P.J., Blobe, G.C. and Hanks, B.A. (2018), "Stromal fibroblasts mediate anti-PD-1 resistance via MMP-9 and dictate TGFbeta inhibitor sequencing in melanoma", *Cancer Immunol. Res.*, **6**(12), 1459-1471. https://doi.org/10.1158/2326-6066.CIR-18-0086.
Zhou, R., Xu, L., Ye, M., Liao, M., Du, H. and Chen, H. (2014), "Formononetin inhibits migration and invasion of MDA-MB-231 and 4T1 breast cancer cells by suppressing MMP-2 and MMP-9 through PI3K/AKT signaling pathways", *Horm. Metab. Res.*, **46**(11), 753-760. https://doi.org/10.1055/s-0034-1376977.
Zhu, H.F. and Li, Y. (2018), "Small-Molecule Targets in Tumor Immunotherapy", *Nat. Prod. Bioprospect.*, **8**(4), 297-301. https://doi.org/10.1007/s13659-018-0177-7.

JL

Abbreviations

RCC	renal cell carcinoma
ccRCC	clear cell renal cell carcinoma
TCGA	The Cancer Genome Atlas
OS	overall survival
PFS	progression-free survival
HE	hematoxylin and eosin
IHC	immunohistochemistry
qRT-PCR	quantitative real-time PCR
EMT	epithelial-mesenchymal transition
P3H4	the prolyl 3-hydroxylase family member 4
GDF15	Growth differentiation factor 15
rhGDF15	GDF15 recombinant human protein
MIC-1	macrophage inhibitory cytokine-1
MMPs	Matrix metalloproteinases